Feasibility Assessment for Amine-Based Shipboard Carbon Capture

by

Stefano Pineda
B.S., Mechanical Engineering
United States Naval Academy, 2019

SUBMITTED TO THE DEPARTMENT OF MECHANICAL ENGINEERING IN PARTIAL FULFILLMENT OF THE REQUIREMENTS FOR THE DEGREE OF

MASTER OF SCIENCE IN MECHANICAL ENGINEERING
AT THE
MASSACHUSETTS INSTITUTE OF TECHNOLOGY

June 2021

Author ……..
Stefano Pineda
Department of Mechanical Engineering
May 14, 2021

Certified by ……...
Betar M. Gallant
Associate Professor of Mechanical Engineering
Thesis Supervisor

Accepted by ……..
Nicolas Hadjiconstantinou
Professor of Mechanical Engineering
Chairman, Committee for Graduate Studies

Feasibility Assessment for Amine-Based Shipboard Carbon Capture

by

Stefano Pineda

Submitted to the Department of Mechanical Engineering on May 14, 2021
In partial Fulfillment of the Requirements for the Degree of
Master of Science in Mechanical Engineering

ABSTRACT

The International Maritime Organization (IMO) set goals to reduce CO_2 emissions by 40% in 2030 with efforts toward 70% in 2050 when compared with CO_2 released per ton-mile in 2008. Maritime traffic relies on non-renewable energy-dense fossil fuels and alternative energy sources have yet to prove feasible for a large sector of the industry. Shipboard carbon capture systems (SCC) offer a possible solution to maritime CO_2 emissions. Here, MEA-based carbon capture systems are designed and evaluated for a representative ultra large container vessel (RULCV) at various lean and rich amine loading pairs, and for 5 ships representative of various ship size categories with average shaft powers ranging from 36 MW to 256 kW. These test cases are evaluated using Aspen Plus and the Aspen Plus Economic Analyzer. To size components, reboiler duty, reboiler diameter, absorber, height, and absorber diameter are all designed for the system to operate at a 90% carbon capture rate with columns at an 80% approach to flooding. In addition to the absorber and stripper, heat exchangers, pumps, and a compressor are designed for these SCCs. The ship system components are evaluated independently and the overall cost of the system is determined from the sum of constituent costs. The carbon capture cost for these MEA-based systems is calculated at \$100 to \$200 per ton of CO_2.

Thesis Supervisor: Betar M. Gallant
Title: Associate Professor of Mechanical Engineering

Contents

1 Introduction

Permanent ecological and humanitarian damage will become a reality unless we promptly and substantially reduce global greenhouse gas emissions [1]. Atmospheric levels of CO_2, the most abundant greenhouse gas, have grown exponentially since the start of the 19th century [2]. This trend must be reversed to avoid grave consequences. To mitigate damages, the International Maritime Organization (IMO) released a strategy to reduce CO_2 emissions 40% by 2030 and pursuing efforts towards 70% by 2050 compared with 2008 CO_2 intensity (g CO_2 / ton / nautical mile (nm)) for maritime shipping [3]. Further, the United States has committed to reducing greenhouse gas emissions to 50% below 2005 levels by 2030 and 191 nations have signed the Paris agreement thus committing to "holding the increase in the global average temperature to well below 2 °C above pre-industrial levels and pursuing efforts to limit the temperature increase to 1.5 °C above pre-industrial levels" [4-6]. To accomplish these goals, efforts across industries must address greenhouse gas emissions. Maritime vessels account for 2.51% of global CO_2 emissions and this thesis seeks to evaluate amine-based shipboard carbon capture (SCC) as a method to reduce CO_2 emissions in the maritime and shipping industries [3].

1.1 Maritime CO_2 emissions

Reduction of CO_2 emissions in the shipping industry has been considered through lower-carbon or zero-carbon alternative fuels, electrification, and carbon capture [3, 7-9]. Lower-carbon fuels such as liquified natural gas (LNG) and methanol have already started supplementing heavy fuel oil (HFO) in some ships [3]. Hydrogen and ammonia are zero-carbon alternatives that could be used with either fuel cells or internal combustion [3, 7].

Full electrification has been considered; however significant challenges persist regarding energy density and space [7]. Despite these challenges, electrification plays a vital role in hybrid power trains utilizing a diesel-electric configuration [3]. In addition to reducing CO_2 generation, efforts to capture carbon on maritime vessels are also underway [10]. The first small-scale SCC system is to be manufactured and tested in late 2021 by Mitsubishi Shipbuilding prior to installation on a Japanese coal carrier [10]. Similar carbon capture efforts have been constructed at scale for land-based power plants; however, this technology has not yet been implemented on ships [11]. With this transition from land-based operation to ship-based operation in its early stages, more research regarding the feasibility of such systems is needed.

Here we consider the design of carbon capture systems for five categories of ships: representative ultra large container vessel (RULCV), large-sized container ships, medium-sized cargo ships, utility ships, and small crafts. These categories are derived from ship data included in ref. [7]. The data are summarized in Table **1.1.1**. The RULCV is based off of the Emma Maersk which is shown in Figure 1.1.1.

Figure 1.1.1 – Image of the Emma Maersk, the largest ship ever built when she was launched in 2006 [12].

Table 1.1.1 – Ship specifications and average CO_2 emissions by grouped categories [7].

		Individual ship specifications			Summary group averages		
		Length (m)	Engine power (kW)	Avg shaft power (kW)	Group shaft power (kW)	CO_2 emissions ($kgCO_2/s$)	CO_2 emissions (t/day)
Container	Emma Maersk (Container)	397	80,080	36,100	23,727	1.73	149.65
	Colombo Express (Container)	335	68,640	34,600			
	Capricorn (Container)	119	3,800	480			
Cargo	Pride of Hull (Cargo/Passenger)	215	37,800	20,000	6,795	0.50	42.86
	Spiegelgracht (Cargo)	168	12,060	3,250			
	Atlantic Klipper (Cargo)	165	14,280	3,500			
	Atlantic Dawn (Crude Oil)	112	4,000	430			
Utility	Maersk Frontier (Offshore Suppy)	83	5,370	1,770	1,055	0.08	6.65
	Alfa Nero (Luxury Yacht)	82	6,900	229			
	Trondheimsfjord 2 (High speed Pass)	25	1,620	760			
	Trearddur Bay (High speed craft)	21	1,800	1,460			
Small Craft	Zalophus (Ferry)	47	800	485	256	0.02	1.61
	Northwestern (Fish/Crab)	38	950	267			
	Hein Senior (Trawler)	24	224	16			

While some ships have shorter trip durations and varied shaft powers throughout their voyages the averages are calculated based on total distance and time at sea [7]. Maximum ship power is generally reported without any average or standard operating power. These reported powers do not accurately represent operating power because power output scales roughly with velocity cubed [13]. The average shaft powers for ships in **Table 1.1.1** are calculated by scaling the maximum power with a load factor as shown in Equation 1.1.1 and Equation 1.1.2 [7].

Equation 1.1.1 $$Load\ Factor\ (LF) = \left(\frac{Average\ Speed\ [kts]}{Max\ Speed\ [kts]}\right)^3$$

Equation 1.1.2 $$Average\ Shaft\ Power\ [kW] = LF\ \times\ Max\ Power\ [kW]$$

Figure 1.1.2 shows the daily CO_2 emissions for these five categories of ships in metric tons assuming non-stop operation at the average shaft powers listed in **Table 1.1.1**.

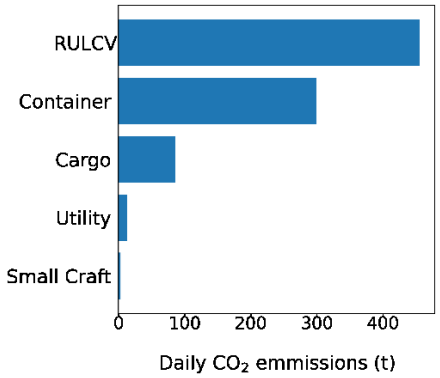

Figure 1.1.2 – Carbon emissions of ship categories from Sandia National Labs and a representative ultra large container vessel (RULCV) motivated by the Emma Maersk at 36 MW shaft power [7].

This assumption of non-stop operation applies well to larger ships that frequently travel hundreds of nautical miles; however, the assumption may overestimate carbon emissions of smaller vessels that do not frequently continuously for twenty-four hours.

1.2 Amine-based shipboard carbon capture (SCC)

The proposed carbon capture systems have already been implemented successfully at scale in land-based carbon capture applications [11]. The technology is mature and of potential

interest for carbon capture on shipboard applications given comparable power requirements of many large vessels to the power plant capacities already tested for CO_2 capture (~10s of MW). However, a unique challenge for shipboard capture is the particular size, weight, and stability constraints. A simple schematic of a land-based amine-based carbon capture system is shown in Figure 1.2.1.

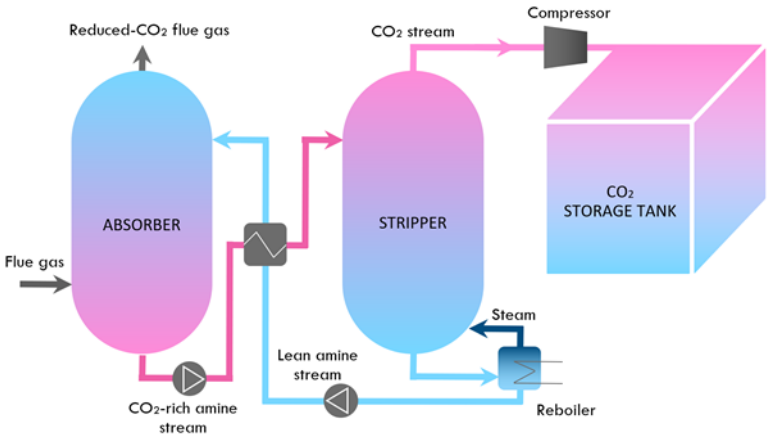

Figure 1.2.1 – Schematic of minimal CCS [14].

Amine-based carbon capture systems function by cycling an amine-containing aqueous solution (30% monoethanolamine (MEA), 70% water) between an absorber column and a stripper column. CO_2 is captured from flue gas (12-13% CO_2 by mass, 40-50 °C [15, 16]) in the absorber column, and CO_2 gas is separated to a purified stream from the amine solution in the stripper column at elevated temperature (120 °C [16]) for subsequent compression and storage.

The number of distinct amines viable for carbon capture is rather large with diverse characteristics [17]. They are classified as primary, secondary, or tertiary based on the number of carbon atoms bonded to the nitrogen atom [17]. Primary and secondary amines are more reactive and readily form carbamate than the more stable tertiary amines [17].

MEA is the most common primary amine and it has been used for decades to capture CO_2 [18]. MEA will be the amine of focus in this study. The general CO_2 absorption/desorption reaction is shown in Equation 1.2.1 [18].

Equation 1.2.1 $$CO_2 + 2\,MEA \rightleftharpoons MEACOO^- + MEAH^+$$

Here, a key consideration is that two MEA molecules are required to adsorb one CO_2 molecule.

1.3 Absorber and stripper operation

In the absorber, flue gas rises vertically through a packed column while a 'lean' (unreacted) amine (recirculating from the stripper column) rains down in a cross-flow configuration, absorbing CO_2 from the flue gas. Packing, which is either structured (wire mesh or folded and perforated metal sheets) or random (regular or irregular metal or ceramic shapes), is utilized to increase contact area between the liquid and gas within the column [19]. A section of structured packing is shown in Figure 1.3.1 [20].

Figure 1.3.1 – Stage of Sultzer Mellpak 250 Y/X structured packing [20].

Often redistributors (plates with recessed holes) are placed between sections of packing to redistribute liquid away from column walls and ensure that the liquid drips and spread across the packing evenly (Figure 1.3.2) [19, 21].

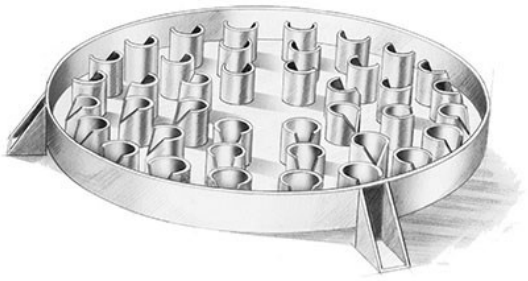

Figure 1.3.2 - Weir-type distributor pan from catalog in ref. [21].

The flue gas exiting the top of the absorber column contains less CO_2 than the entering flue gas due to its chemical reaction with the amine along the absorber flow path, thus the majority of CO_2 exits at the bottom of the absorber column and is in chemisorbed form. This so-called 'rich' amine is then pumped through a heat exchanger and enters the stripper column (entrance temperature 110 °C, 2 bar [22]) where it flows vertically down through the column's packing as warm vapors (heated by a reboiler operating on a slipstream from the power plant turbine) flow upwards. As the amine approaches the bottom of the stripper column, an internal thermal gradient generated by the reboiler (which heats the bottom of the column) progressively heats the amine (exit temperature 120 °C, 2 bar [16, 22]). This heat and the vapors flowing upward through the column facilitate the desorption of CO_2 from the amine. To reduce the amount of heat added by the reboiler [kW], referred to as 'reboiler duty', the hot lean amine exiting the stripper is pumped through a heat exchanger

to pre-heat the rich amine. After preliminary cooling, the lean amine is further air-cooled (omitted from Figure 1.2.1) prior to entering the absorber (40 °C [16, 22]) to capture CO_2.

In the stripper and the absorber, gas flows are driven by pressure differentials. In the absorber, the CO_2-lean exhaust exiting the top of the column is vented to the atmosphere at ambient pressure and the entire absorber column operates just above ambient pressure [16, 22]. In the stripper, the exhaust gas exiting the top of the column, comprised mostly of CO_2 and water vapor, is first cooled (18 °C, 2 bar [16, 22]) to condense liquid water and compress CO_2 for storage. The liquid water is then recycled back into the absorber feed stream [16]. In practice, the liquid water first passes through a throttling valve to reduce pressure.

These two columns and the infrastructure to support a carbon capture plant demand sufficient space, weight capacity, and energy from any ship on which they are installed. The space and weight capacity come with significant costs to the carrying capacity of shipping vessels in terms of twenty-foot equivalent unit containers (TEU), bulk cargo, fossil fuels, or other specialized cargo. The energy requirements are critical to define because the desorption process demands a significant fraction of the energy spent to regenerate the lean amine. With these added constraints in an industry already pressed by narrow profit margins, a thorough understanding of carbon capture systems' footprints on ships must be developed in order to justify overhauls and retrofits of existing and new ships [23].

1.4 General system parameters

In this work, to provide a representative assessment relevant to current capture technology, the amine was selected to be MEA. MEA is a commonly-used amine for CO_2 capture and its behavior in CCS is well understood [8, 9, 16, 22, 24]. The basis of this system is adopted from ref. [16, 22] and it is further discussed in chapter 2 . MEA chemistry, kinetic parameters, and transport properties for various chemical components are taken from ref. [22] and shown in Table **1.4.1** and Table **1.4.2**. Some of these equations appear unbalanced as they are reproduced directly from Aspen Plus documentation [22] in which standard notation for 'MEA' will vary in the number of implicit hydrogens depending on whether 'MEA' is in lean or carbamate / ammonium form; in practice all reaction are mass balanced. Generally, the Aspen Plus simulation in ref. [22] is used as a starting point, and unused streams and components around the absorber and stripper columns are deleted as described in subsequent text.

Table 1.4.1 – Globally defined equilibrium reactions from ref. [22].

Reaction type	Reaction
Equilibrium	$2H_2O \leftrightarrow H_3O^+ + OH^-$
Equilibrium	$CO_2 + 2H_2O \leftrightarrow HCO_3^- + H_3O^+$
Equilibrium	$HCO_3^- + H_2O \leftrightarrow CO_3^{2-} + H_3O^+$
Equilibrium	$MEAH^+ + H_2O \leftrightarrow MEA + H_3O^+$
Equilibrium	$MEACOO^- + H_2O \leftrightarrow MEA + HCO_3^-$

Table 1.4.2 – Stripper and absorber chemical reactions from ref. [22].

Reaction type	Reaction
Equilibrium	$MEAH^+ + H_2O \leftrightarrow MEA + H_3O^+$
Equilibrium	$2H_2O \leftrightarrow H_3O^+ + OH^-$
Equilibrium	$HCO_3^- + H_2O \leftrightarrow CO_3^{2-} + H_3O^+$
Kinetic	$CO_2 + OH^- \rightarrow HCO_3^-$
Kinetic	$HCO_3^- \rightarrow CO_2 + OH^-$
Kinetic	$MEA + CO_2 + H_2O \rightarrow MEACOO^- + H_3O^+$

Kinetic	$MEACOO^- + H_3O^+ \rightarrow MEA + CO_2 + H_2O$

Within the columns of this model, a structured Sulzer Mellapak 250 Y packing from the catalog in ref. [20] (Figure 1.3.1) is used [22]. This is a corrugated metal packing with holes and is the most widely used structured packing worldwide [20]. The packing functions to increase interfacial area of the liquid to increase the rate of adsorption and desorption in the columns. This packing is tailored particularly well for vacuum to moderate pressure applications and is typically used in absorbers and strippers in addition to many other use cases [20]. Structured packing, as opposed to random packing, is used for its low pressure drop and relative high capacity relative to diameter [25]. The number of stages is set to 20 and these stages represent the 20 sections of packing physically in the column and independently simulated [22].

To determine the height and diameter of the columns, the columns are sized to the typical design parameters for land-based CO_2 capture of 90% CO_2 removal at the absorber outlet, and 80% 'approach to flooding' [8, 9, 19, 25]. Flooding is a phenomenon in which the gas flow velocity meets or exceeds the velocity of droplets in a column causing the column to fill with liquid and bubble or spray out the top [25]. The approach to flooding is defined by the ratio of the gas velocity (u_v) to the velocity at which flooding would occur (u_f) as shown in Equation 1.4.1. The gas velocity can be approximated by dividing the volumetric flow rate of the gas (Q) by the effective cross-sectional area of the column (a_c) (area of unimpeded passage) as shown in Equation 1.4.2.

Equation 1.4.1 $$Approach\ to\ flood = \frac{u_v}{u_f}$$

Equation 1.4.2

$$u_v = \frac{Q}{a_c}$$

In common operation, 0.8 is selected to provide an adequate margin of safety to avoid such risk [19]. Normal and flooding operation of a column are depicted in Figure 1.4.1.

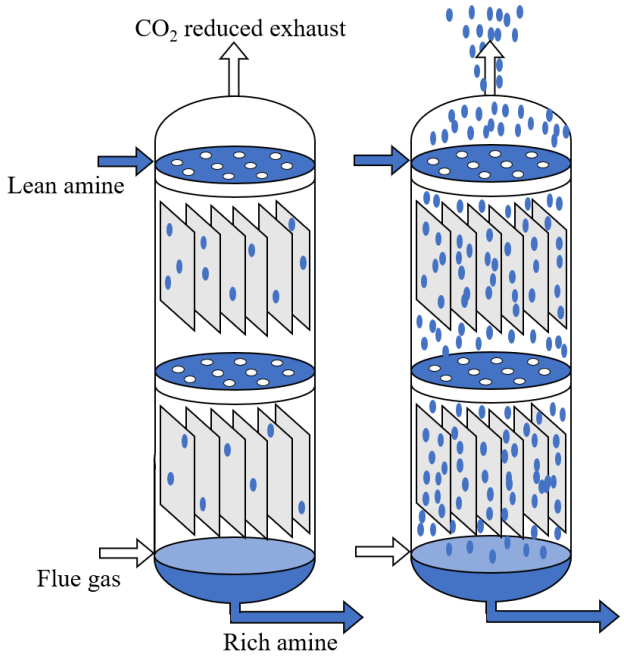

Figure 1.4.1 – Left - Normal ($u_v < u_f$ - no fluid flowing up to top of column), **Right -** Flooding ($u_v > u_f$ - lean amine sprays out with the exhaust) operation of a 2-stage absorber column with structured packing.

For a given set of flow rates, the carbon capture percentage is largely determined by the height of the column, while the percent approach to flooding is mostly determined by the diameter. The height of packing needed (Z) can be estimated by Equation 1.4.3 [26].

Equation 1.4.3

$$Z = \frac{G_m}{K_L \alpha C_t} \int_{y2}^{y1} \frac{dy}{y - y_e} \quad [26]$$

Where (G_m) is a molar gas flow rate, (K_L) is the overall gas phase mass transfer coefficient (α) is the interfacial surface area per unit volume, (C_t) is molar concentration, (y_e) is the equilibrium mole fraction of solute in gas at any point, and (y_1 / y_2) are mole fractions of

the solute in gas at the bottom and top of the column respectively [19, 26]. The column diameter (D_c) can be estimated with Equation 1.4.4 [19, 27].

Equation 1.4.4

$$D_c = \sqrt{\frac{4\hat{V}_w}{\pi \rho_v \hat{u}_v}}$$

Here ($\hat{V}_w$), the maximum vapor flow rate, the vapor density (ρ_v), and the maximum allowable vapor velocity ($\hat{u}_v$) determine the approximate column diameter. This approach can give a first estimate for column diameter before detailed design via simulation. Because this equation considers the maximum allowable vapor flow rate, it already has an assumption regarding flooding built in where the maximum allowable flow rate is determined by a 100% approach to flooding.

The percent approach to flooding affects the efficiency of CO_2 adsorption and desorption. At higher percentage approach to flooding, higher gas velocities increase mixing and enhance contact area between liquid and gas; however, they also decrease the amount of time spent at a given height in the column. A simple approach to column stage efficiency (E_{mv}) is shown in Equation 1.4.5.

Equation 1.4.5

$$E_{mv} = \frac{y_n - y_{n-1}}{y_e - y_{n-1}}$$

Equation 1.4.5 shows the efficiency as a function of CO_2 (or solute) concentration (y) at a given stage (n), equilibrium concentration (y_e), and the CO_2 concentration of the previous stage (y_{n-1}) [19]. Naturally, the rate at which solute concentration approaches equilibrium has kinetic dependencies which are affected by the flow rates, and the percentage approach to flooding. Since the efficiency of column stages and the percentage approach to flooding (the ratio gas velocity to max velocity allowable) are coupled through these mixing effects, the approach to flooding and column height and diameter should be considered together. Another simpler method for estimating stage efficiency (E_0) is the O'Connel method in

which only the molar average liquid viscosity (μ_a) and the average relative velocity of the light (or gaseous) component (a_a) are used as shown in Equation 1.4.6 [19].

Equation 1.4.6 $$E_0 = 51 - 32.5 \log(\mu_a a_a)$$

To address the issue of coupled height and diameter in the absorber and coupled diameter and reboiler duty in the stripper, this work iteratively solves for both height and diameter in the absorber, and diameter and reboiler duty in the stripper to meet both the flooding and carbon capture constraints in the columns.

'Flue flow rate' (the mass flow rate of exhaust gas entering the absorber column) is a critical input to size columns. Flue flow and CO_2 flow are obtained from ship data as discussed in section 2.2 and are taken in this thesis as inputs and constraints on the model. The flue flow rate for a particular ship then determines the needed amine flow rate to remove the desired amount of CO_2 and achieve the pre-selected amine loading in the absorber and stripper. The amine loading, *AL,* is defined in Equation 1.4.7. It is a ratio of all carbon-containing species to the MEA-containing species within the amine solution, which includes some portions of unreacted (physisorbed) CO_2 in addition to predominantly chemisorbed CO_2 bound to the amine as indicated. Some CO_2, upon hydrolysis of the MEA-CO_2, will wind up as bicarbonate (HCO_3^-) or carbonate (CO_3^{2-}) ions (see Table **1.4.1** and Table **1.4.2**) and are also counted in this loading ratio.

Equation 1.4.7 $$AL = \frac{[CO_2]+[HCO_3^-]+[CO_3^{2-}]+[MEACOO^-]}{[MEA]+[MEAH^+]+[MEACOO^-]}$$

The difference between the rich (AL_R) and the lean (AL_L) amine loading is the loading delta, or Δ_{AL}, as shown in Equation 1.4.8.

Equation 1.4.8 $$\Delta_{AL} = AL_R - AL_L$$

For a given CO_2 molar flow rate ($\dot{n}_{CO_2}$), the loading delta (a design constraint since both the rich and lean loadings are defined as inputs) determines the necessary molar amine flow rate ($\dot{n}_{MEA}$).

Equation 1.4.9 $$\dot{n}_{MEA} = \frac{\dot{n}_{CO_2}}{\Delta_{AL}}$$

These flow rates are then simulated in accordance with the methodology delineated in chapter 2 to appropriately size the columns.

2 Methodology

In this section validation, system design, system inputs, absorber and stripper column sizing, and economic analysis process are presented.

2.1 Validation

To simulate the carbon capture process, a template provided in Aspen Plus documentation was first considered [22]. The MEA-based Kaiserslautern pilot plant available in Aspen Plus documentation has been thoroughly simulated and validated elsewhere against data from the plant [16, 22]. This file is available as an example in Aspen Plus V11.0 as "ENRTL-RK_Rate_Based_MEA_Model". It is "meant to be used as a guide for modeling the CO_2 capture process with MEA" and "as a starting point for more sophisticated models for process development" [22]. Under these operating conditions, the plant captures 72.6% of the CO_2 from a gas burner [22, 28]. The absorber can handle flue gas flow rates from 30 to 150 kg/h and the referenced simulation models the plants operation with 72 kg/h of flue gas [22, 28]. This CCS process utilizes an absorber and stripper that are 4.25 m and 2.55 m tall, respectively [16, 22]. Both columns have 0.125 m diameters [16, 22]. These dimensions need to be adjusted to system-specific flowrates, however, this model is often used as a base model for MEA-based CCS simulations [29-32]. The Aspen plus flowsheet of the Kaiserslautern CCS is shown in Figure 2.1.1.

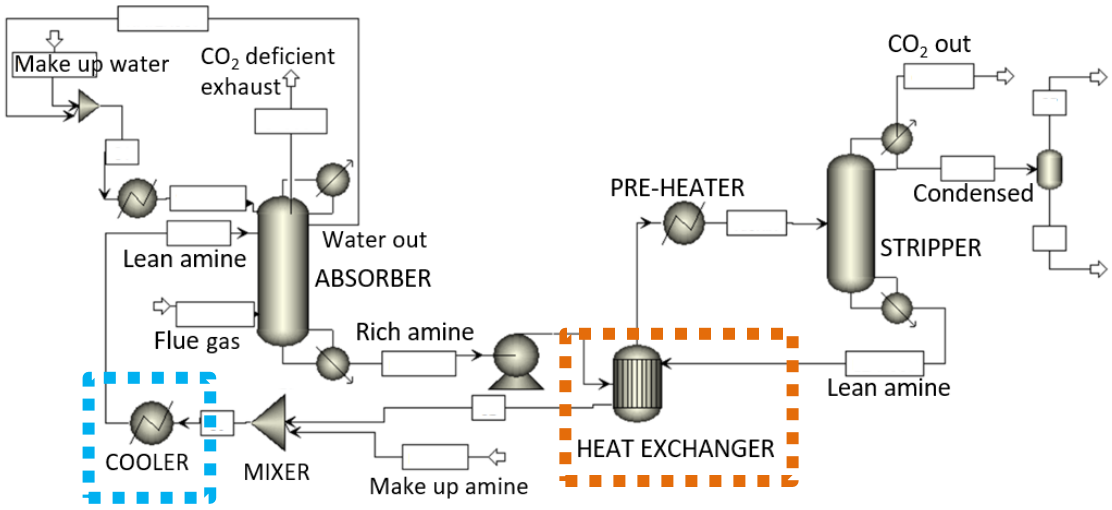

Figure 2.1.1 – Kaiserslautern pilot plant CCS rendered in Aspen Plus from "ENRTL-RK_Rate_Based_MEA_Model" template provided in Aspen Plus documentation (schematic generated in house) [22].

Convergence time, defined here as the time d to reach a solution to the system of equations governing the processes within an Aspen Plus simulation, can be prohibitively long in larger systems, especially those containing loops where solutions depend on multiple interdependent component outputs. This system includes 10 components and converges quickly when it is initialized with ideal stream values and component sizes derived from the plant's actual operating values. Upon varying flow rates and system sizing slightly, the simulation's time-to-convergence drastically increases. Upon slightly larger increases in flow rates, for example, a 2% increase for the flue flow rate, the simulation no longer converged. Convergence with this new flow rate required resizing multiple components and adjusting other flow rates simultaneously: a time-intensive and iterative process. It is also noted that some approximations in Aspen Plus modeling may be required to achieve realistic system performance. For instance, make-up streams labelled WATERMU and

MEAMU in Figure 2.1.1, representing additional water and amine inputs, were not implemented in the pilot plant, but were found to be necessary to achieve mass balance and to facilitate convergence of the model [22]. These parameters without physical basis in the plant also need to be adjusted manually to converge models of this size and complexity [22].

Therefore, to avoid iteratively adjusting the parameters of individual components to reach overall system convergence in this work, the stripper and absorber units were isolated for subsequent modelling as subsystems. Converged results of the isolated units were then compared with those of the entire system to ensure extra error was not introduced. This approach was found to effectively distill the physicochemical, kinetic, and energetic performance of the capture system while dramatically shortening simulation times. To generate these isolated results, the stripper and absorber inlet streams from the Kaiserslautern pilot plant's converged solutions were set as the inlet streams into the isolated stripper and absorber. Isolated absorber and stripper units as used in this work are shown in Figure 2.1.2.

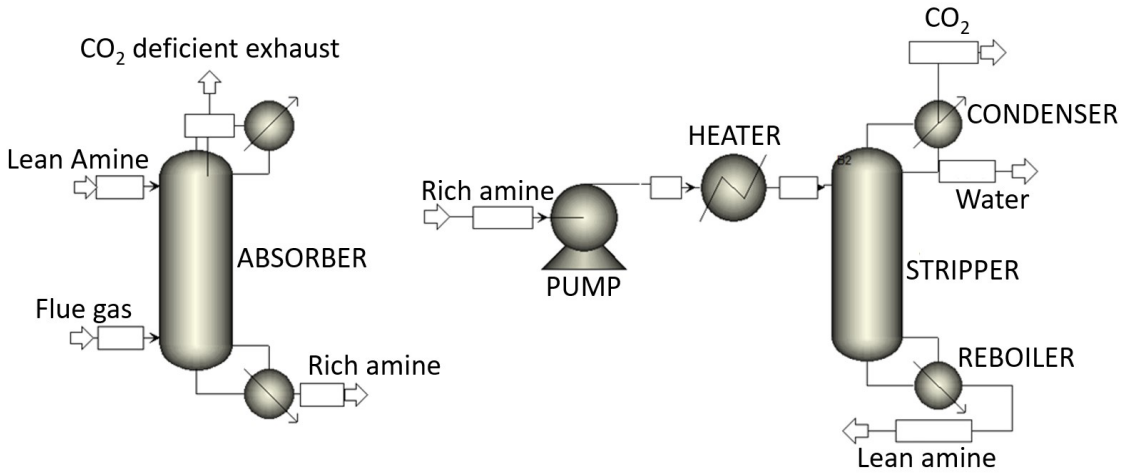

Figure 2.1.2 - Isolated absorber (left) and stripper (right) flowsheets as used in this thesis.

In these simplified models, since the stripper and absorber are no longer connected by a heat exchanger, a preheater was instead introduced to account for the heating normally done by the heat exchanger on the inlet stream to the stripper in the integrated system. This preheater was not counted towards the energy required to desorb CO_2 in the stripper unit as this heating is typically done using a heat exchanger internal to the system. These two units are more forgiving with convergence and can be adjusted more rapidly to a set CO_2 capture rate and lean-rich loading pairs.

In Figure 2.1.1, the LEANIN and WATERIN streams from are combined into one feed stream. In the Kaiserslautern pilot plant, WATERIN and LEANIN enter below stages 1 and 3 respectively, whereas the isolated absorber has both streams premixed entering below stage 1 [16]. To evaluate the impact of this assumption, the amine loadings and carbon

capture rate for the isolated absorber and the Kaiserslautern absorber are compared in Table 2.1.1.

Table 2.1.1 – Amine loading and CO_2 capture comparison for Kaiserslautern absorber and isolated absorber model.

ABSORBER	Kaiserslautern simulation [22]	Isolated simulation	% error $\frac{\lvert Kaiserslautern - Isolated \rvert}{Kaiserslautern}$
Lean loading (mol CO_2/mol MEA)	0.245	0.244	0.526
Rich loading (mol CO_2/mol MEA)	0.355	0.355	0.0761
% CO_2 removal	72.6	73.6	1.33

The results indicate that, by integrating the lean amine and water inlets in the simplified model, the lean loading increases by less than 1% while the rich loading remains nearly unchanged. Notably, because the lean amine enters the isolated absorber column two stages physically above where it enters in the Kaiserslautern absorber, a marginally larger percentage of the CO_2 is removed from the flue gas. The difference is small (<1%) and directly related to an increase in the functional height for absorption. As the lean amine flows past the flue gas for a larger vertical distance (corresponding to an additional 42 cm of contact length), more CO_2 is absorbed into the amine. With such small variations between the relevant parameters of the absorbers when the inlet stream locations are varied, we conclude that the isolated approach to simulating an absorber column for carbon capture appears valid. We now proceed to use this framework to estimate column sizing, CO_2 capture percentages, energy requirements, and economic costs for these isolated

components. It is noted that future work, beyond the scope of this thesis, may need to examine and optimize the ideal stages of entry for lean amine and water for further-refined modeling and possible additional process gains.

Next, to validate that the isolated stripper will generate similar results to the stripper connected to other units, exact compositions and flow rates from the Kaiserslautern model are first used, before varying them in later sections. The rich amine composition and flow rates are identical in both cases. Since the isolated stripper column had the exact same chemistry, dimensions, condenser, and reboiler, the output from the isolated stripper is identical to that of the Kaiserslautern stripper. Since no parameters, such as feed inlet stage for the absorber, were varied for the stripper, it is replicated directly as an isolated stripper to be adjusted for various carbon capture system sizes.

2.2 Stream inputs

To size columns for shipboard carbon capture, the engine operating conditions are needed. These data are sourced from [7] which compiled data for thirteen representative ships. Given the ship's cruising shaft power, the ship's CO_2 emissions can be approximated using a factor of 73 g CO_2 released per megajoule of energy released [33]. Equation 2.2.1 shows how the mass flow of CO_2 ($\dot{m}_{CO2}$) is calculated from the ship's power (P), the CO_2 per unit energy (ρ_{CO2}), and the ship's thermal efficiency (η).

Equation 2.2.1 $$\dot{m}_{CO2} = P * \rho_{CO2} * \eta^{-1}$$

With the flow rate of CO_2, the total flue flow rate and component flow rates are calculated using diesel fuel flue gas compositions (12.57% CO_2 by mass) [15]. The flue flow rate for

the largest ship considered (a representative ultra large container vessel (RULCV) inspired by the Emma Maersk) was determined to be 28 kg/s while the small ship category releases 0.1 kg/s. By comparison, even the small ship category produces five times the flue gas of the Kaiserslautern pilot plant whose gas burner generates flue gas at 0.02 kg/s.

With a determined CO_2 flow rate in the flue gas, Equation 1.4.9 is used to calculate the necessary MEA flow for a given amine loading delta desired. Since SCCs are generally designed to capture 90% of the CO_2 in the flue gas, the designed MEA flow rate is calculated accordingly [8, 9]. We here recall that the amine solution is 30% MEA and 70% water by mass as this ratio is close to optimal for minimizing reboiler duty [24].

The stripper unit for each design is simulated before the absorber to provide lean loading molar compositions that specify the absorber output. Rich loading molar compositions are approximated by using Equation 1.4.7, an assumption that $[\mathrm{MEAH^+}] = 1.2 * [\mathrm{MEACOO^-}]$, and that the 30% percent MEA by weight is 11% molar [22]. In the converged solution to the Kaiserslautern pilot plant model, the ratio of $[\mathrm{MEAH^+}]/[\mathrm{MEACOO^-}]$ in the rich amine stream is approximately 1.2, therefore this ratio is built into these simulations. This ratio is used to initialize the rich amine stream entering the stripper before the Aspen Plus calculates equilibrium concentrations based on the equilibrium equations. These starting assumptions are then varied until the rich amine loading converges on the desired amine loading in Aspen Plus. The molar composition inputs needed to reach these rich loadings are listed in Table 4.6.1. Since MEA can only physically absorb up to an amine loading of 0.5, amine loadings greater than 0.5 require CO_2 stored in the form of carbonate,

bicarbonate, or physisorbed CO_2. To account for this behavior, rich loadings greater than 0.5 are initialized with bicarbonate.

2.3 Column parameters and sizing

The same 250Y packing used in the Kaiserslautern validation is used in the isolated absorber and stripper as this structured packing provides low pressure drops and high flow capacity for a set column diameter [16, 22, 25]. 20 stages are used for both the stripper and the absorber and the height of the strippers in this thesis are assumed to be 6.5 m in accordance with ref. [8]. The stripper height is another variable that can be optimized though it is taken as a constant in this study to reduce the parameter space. With the goals of an 80% approach to flooding, and a 90% CO_2 capture rate, diameter and reboiler duty are the two most critical parameters that control these outputs. The reboiler duty controls CO_2 desorption (capture rate) and steam generation, while the diameter determines the cross section through which these vapors will rise (flooding). Stripper pressure is set to 2.5 bar while the absorber pressure is set at 1 bar [34]. By operating the absorber at ambient pressure, flue gas can flow in without compression. The flue gas, lean amine, and rich amine all enter the isolated absorber and stripper at 40°C. The lean amine temperature is obtained from the Kaiserslautern simulation.

The stripper is designed (diameter, reboiler duty, and distillate rate) first because rich amine molar composition inputs are known from Table 4.6.1. This rich amine enters a pump and is compressed from 1 bar to 2.5 bar. The preheater then heats the amine to 95 °C: a conservative estimate based on simulations using the heat exchanger model in Figure 2.4.1.

The stripper's condenser is set to 18 °C and both reboiler duty and column diameter are iteratively varied until 90% of the CO_2 entering the absorber flows out the stripper's condenser. The column diameter is simultaneously varied to keep the column at an 80% maximum approach to flooding [19, 25]. This process gives the required reboiler duty and column diameter to capture 90% of the CO_2 and operate at an 80% approach to flooding.

Sizing the absorber begins with lean amine molar compositions from the stripper simulation and appropriate flow rates. The height and diameter of the absorber column are then iteratively varied until the column operates at an 80% maximum approach to flooding and 90% rate of CO_2 capture.

2.4 Economic analysis

To account for other major system costs such as heat compressors, pumps, and heat exchangers, these components are simulated separately for sizing and economic analysis. With columns sized and reboiler duties determined, the heat exchangers and compressor are sized for the system flow rates. The heat exchanger relies on the amine flow rate while the compressor sizing depends only on the CO_2 capture rate which is a direct function of the ships' power in this model.

When simulating the absorber and stripper pair separately, the heat exchanger must be replaced by another heat source to analyze the operating and capital costs of the system. Here a simple heater is used to preheat the rich amine. To size and evaluate the cost of the heat exchangers a separate simulation is conducted on just the heat exchangers with water

as the working fluid. The first heat exchanger preheats the rich amine (95 °C) while the second heat exchanger is an air-cooled head exchanger that reduces the lean amine temperature prior to it re-entering the absorber (40 °C). The heat exchanger setup is shown in Figure 2.4.1. The "lean" and "rich" amine streams are denoted with quotations to indicate that water is used the working fluid for the sizing of these heat exchangers.

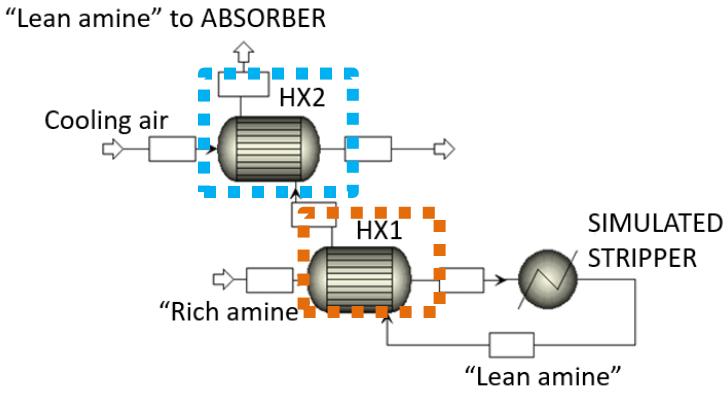

Figure 2.4.1 – Heat exchanger cost evaluation using a simple heater to avoid convergence issues common when sizing stripper reboilers with dependent heat exchangers.

The heat exchanger with the rich stream entering (40-50 °C) preheats the rich amine (95 °C) before entering the simulated stripper. The simulated stripper heats the rich amine to the same exit temperature as the stripper (129 °C). After passing through the first heat exchanger, the lean amine passes through an air-cooled heat exchanger prior to entering the absorber. The air-cooled heat exchanger cools the working fluid to 40 °C.

To compress the CO_2 that has been removed in the stripper, an isolated compressor is simulated as shown in Figure 2.4.2.

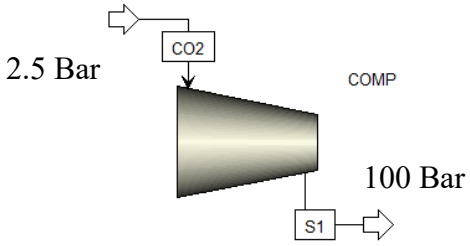

Figure 2.4.2 – Compressor.

The compressor increases the pressure of the CO_2 stream for storage in an onboard tank at 100 bar [8]. The compressor is modelled using the isentropic method and the Aspen Plus default compressor efficiency of 0.8.

With the absorber, stripper, heat exchangers, and compressor all converged, the Aspen Plus Economic Analyzer (APEA) is utilized to generate cost estimates for capital (CAPEX) and operating (OPEX) expenditures for each of the components within the models. The costs of the absorber, stripper, pump, and heat exchangers are included in the analysis while the costs of the preheater (Figure 2.1.2) and the simulated stripper (Figure 2.4.1) are omitted.

To generate an annual cost of operations (*A)*, the upfront capital expenditures (*P*) are converted into and annualized cost using Equation 2.4.1.

Equation 2.4.1 $$A = P\frac{[i(1+i)^n]}{[(1+i)^n-1]}$$

An interest rate of 8% and a 20-year term are assumed to generate the annualized expenses for each carbon capture installation [8]. To calculate the carbon capture cost (CCC) of the system, the sum of the annualized CAPEX and the OPEX is divided by the total tons of CO_2 captured by the CCS each year. It is assumed that the ship operates 24/7 for the entire year for the purposes of calculating the CCC. This is a reasonable assumption for larger

ships that often travel between distant ports; however, for the smaller ships, it may overestimate the total CO_2 produced and underestimate the CCC.

2.5 Parametric sweep of amine loadings

Operating the absorber and stripper at appropriate rich and lean loadings is critical to optimize reboiler duty, amine flow rates, and component sizing. Amine concentration, stripper pressure, and lean solvent loading are key parameters affecting the capital and operating costs [24]. For MEA the ideal amine concentration is approximately 30% MEA by weight [24]. Higher stripper pressures reduced total equivalent work of carbon capture systems as less heat contributes to the vaporization of water and more contributes directly to CO_2 desorption; however, at higher pressures the required stripper temperature increases. To avoid thermal degradation of amines and components, the stripper pressure is herein set to 2.5 bar, the maximum considered in previous work, as higher pressures would increase the stripper operating temperature [35]. Lean loadings of 0.1, 0.125, 0.15, 0.175, and 0.2 were tested with rich loadings of 0.45, 0.475, 0.5, and 0.525. These low lean amine loadings were selected because Xue et al. showed a minimum for reboiler duty at a lean amine loading of 0.17 with 30 weight percent MEA and a stripper pressure of 1.5 bar [24]. The high rich amine loadings were based on preliminary calculations indicating that higher rich loading reduce the carbon capture cost. Ranges of lean loadings above the list considered and rich loadings below those considered in this thesis are also typical and should be considered in future work [8, 9]. For each of the twenty amine loading combinations, the absorber, stripper, heat exchangers, pumps, and compressor were sized to handle half the cruising speed shaft power (18 MW for the lean / rich loading parameter

sweep) of the RULCV inspired by the Emma Maersk: the largest container ship considered in the Sandia national laboratory report on zero emission vessels [7].

2.6 Testing ship categories

To evaluate feasibility of CCS on ships smaller than an ULCV, four ship categories from the Sandia report are considered [7].

Table **1.1.1** shows the ships, their lengths, engine power, average shaft power, and group averages for CO_2 emissions. The average shaft power data for each ship is derived from actual ship voyages reported on marinetraffic.com [7]. From voyage duration and distance, the maximum ship power (MCR) is scaled to an average power as shown in Equation 2.6.1 [7].

Equation 2.6.1 $$Average\ Shaft\ Power\ [kW] = \left(\frac{Average\ Speed\ [kts]}{Max\ Speed\ [kts]}\right)^3 \times MCR$$

Using these average shaft powers, amine flow rate is calculated in accordance with Equation 1.4.9 and the amine loading delta. The rich amine loading is set to 0.5 and lean loading is set to 0.17 [24].

3 Results

3.1 RULCV stripper

The amine flow rate in the CCS is inversely proportional to the amine loading delta defined for a given amine loading pair. With a lean amine loading of 0.2 and a rich amine loading of 0.45, the loading delta is 0.25. Dividing a CO_2 flow rate by the loading delta determines the needed amine flow rate. If the loading delta doubles, the needed flow rate will be reduced by a factor of two. The relationship for the range of tested amine loadings can be seen in Figure 3.1.1.

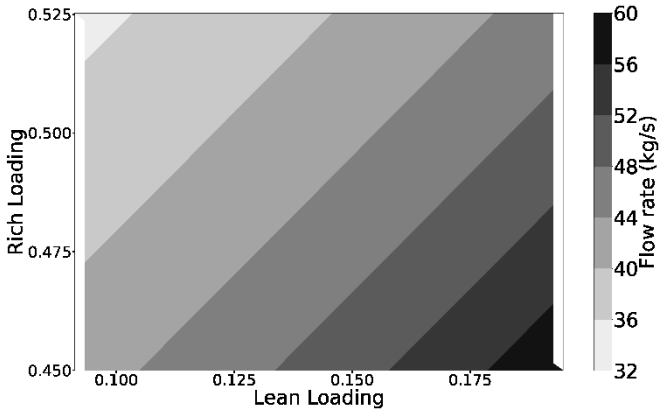

Figure 3.1.1 - Amine flow rate required to remove 90% CO_2 from the flue gas of a RULCV, calculated using Equation 1.4.9.

The rich loadings are set as inputs to the simulations and the lean loadings are an output that varies with column diameter and reboiler duty. The lean loading outputs are all lower than the anticipated lean loading values by approximately 0.006 mol CO_2 / mol MEA. The range of lean loading values that are offset in Figure 3.1.1 depicts this result. The offset of the lean loadings is a result of inconsistent preliminary rounding for the initialization of

rich amine streams. The amine solution intended to be 30% by mass MEA was rounded to 11% MEA molar as opposed to remaining at 11.22% MEA molar. The reboiler duties required to desorb the CO_2 at various amine loading pairs are shown in Figure 3.1.2.

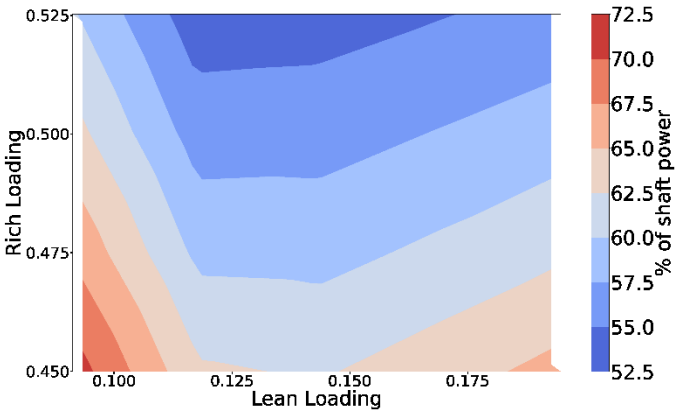

Figure 3.1.2 – Stripper reboiler duty as percentage of RULCV cruising shaft power (18 MW).

The contour of reboiler duty shows that higher rich loadings require less heat to desorb CO_2. Meanwhile, for a fixed rich loading, as lean loading decreases (requiring further extent of CO_2 removal from amine in the stripper), the reboiler duty also decreases until a critical lean loading around 0.13 for all cases, where further decreases in lean loading increase necessary reboiler duty. This feature has been observed for various amines in other work [24, 35]. This behavior can be explained with the Langmuir model for thermal swing adsorption (TSA). This model describes both chemisorption and physisorption in accordance with Equation 3.1.1 and Equation 3.1.2 [36].

Equation 3.1.1

$$\frac{q}{q_s} = \frac{b_{CO_2} P_{CO_2}}{1 + b_{CO_2} P_{CO_2}}$$

Equation 3.1.2

$$b_{CO_2} = b_0 \exp\left(\frac{-\Delta h}{RT}\right)$$

Here, (q) is the number of occupied sites for CO_2 to adsorb while (q_s) is the total number of sites available. In this CO_2 capture system, the ratio of (q) to (q_s) is effectively the amine loading. In this model, the amine loading is a function of the Langmuir parameter (b_{CO2}) and the partial pressure of CO_2 (P_{CO2}). From Equation 3.1.2 the Langmuir parameter is a function of the heat of adsorption (Δh), temperature (T), the universal gas constant (R), and a constant fit to adsorption data (b_0) [36]. Since desorption is an endothermic process, the heat of adsorption is negative so the Langmuir parameter approaches the adsorption constant as temperature increases. This makes the effective amine loading exponentially decay as temperature increases. The exponential decay releases progressively less CO_2 for each increment in temperature thus a transition point at which further heating yields less CO_2 released per unit of energy input is naturally expected. In Figure 3.1.2 that transition point is likely seen at a lean amine loading of approximately 0.13 for the 2.5 bar stripper pressure.

The temperature in the stripper is largely determined by its operating pressure since liquid water and steam are both present. Therefore, further addition of heat will contribute proportionally more towards steam generation within the stripper than towards CO_2 desorption below the critical amine loading of 0.13.

Because more steam is being generated within the stripper at lower lean loadings, larger diameters are required to maintain the same percent approach to flooding. Here, the contours for stripper diameter exhibit a similar behavior as shown in Figure 3.1.3.

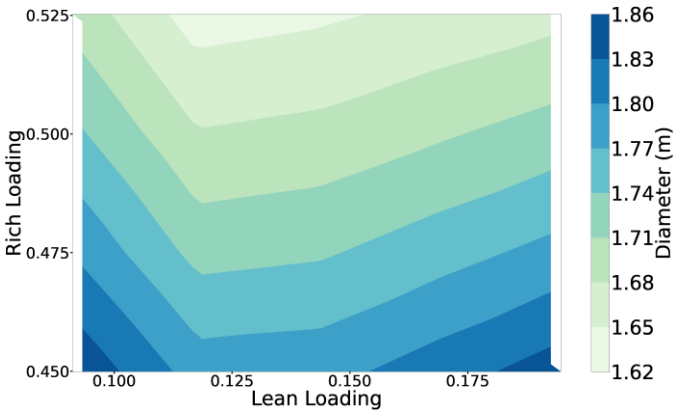

Figure 3.1.3 – Stripper diameter for RULCV sized CCS.

Again, we see that at higher loading deltas, less amine is needed and column diameters are correspondingly smaller. The same transition occurs for very low lean amine loadings; however, it appears lower than 0.13 and possibly closer to 0.12.

3.2 RULCV absorber

The required absorber height for the parametric sweep of amine loadings is shown in Figure 3.2.1.

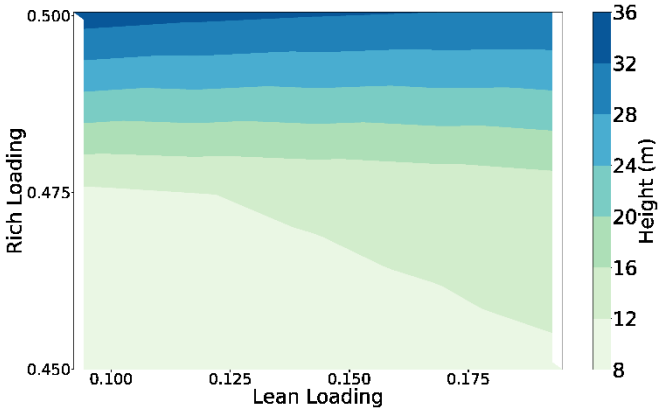

Figure 3.2.1 – RULCV absorber height for designed rich / lean amine loading pairs with constant flue gas flow rate.

The height of the absorber necessary to capture CO_2 increases sharply with amine loadings greater than 0.5 (not shown). CO_2 needs to be stored in carbonate or bicarbonate beyond amine loadings of 0.5. Since this is a less efficient process, the absorber column height increases rapidly approaching and beyond rich amine loadings of 0.5. At an amine loading of 0.525, the heights required for the absorbers are completely unrealistic and infeasible at ambient pressure (131 to 136 m). The absorber height shows slight variation with respect to lean loading. Naturally, starting with more CO_2 in the lean stream will decrease the rate at which CO_2 is absorbed throughout the column. This can be explained with a rate law for reaction kinetics shown in Equation 3.2.1 [37].

Equation 3.2.1 $$\text{Rate} = k[\text{A}][\text{B}][\text{C}]^{-1}[\text{D}]^{-1}$$

Here, (k) is a temperature dependent rate constant for a reaction (CO_2 adsorption in this case), [A] / [B] are concentrations of reactants, and [C] / [D] are concentrations of products. Equation 3.2.1 shows that the speed of the absorption reaction will be faster if there are less of the products and more of the reactants. With a higher lean loading, there is a greater concentration of reactants (namely $MEAH^+$ and $MEACOO^-$) which will reduce the kinetics of the absorption reaction and extend the needed height to fully absorb 90% of the CO_2 present in the flue gas.

The absorber diameters are shown in Figure 3.2.2.

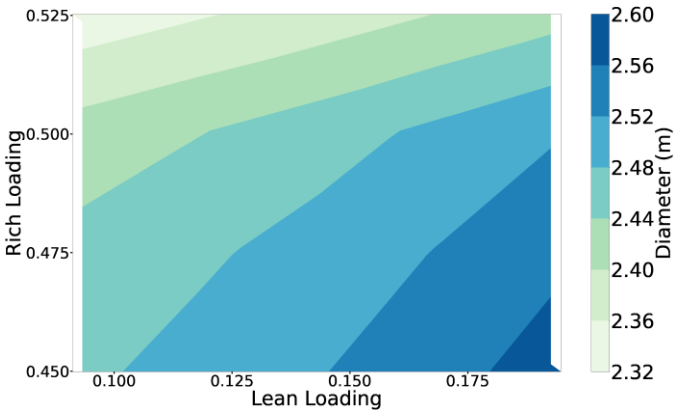

Figure 3.2.2 – RULCV absorber diameter.

Absorber diameter increases with higher lean loadings and lower rich loadings. Similar to the stripper, lower amine flow rate from lower higher loading deltas reduces the required column diameter. This trend mostly follows the amine loading flow rate patterns.

3.3 RULCV economic analysis

With columns, heat exchangers, pumps, and compressor sized to flow rates and operating conditions, the total CAPEX required for the system installation is calculated. Figure 3.3.1 shows the CAPEX for the Emma Maersk CCS.

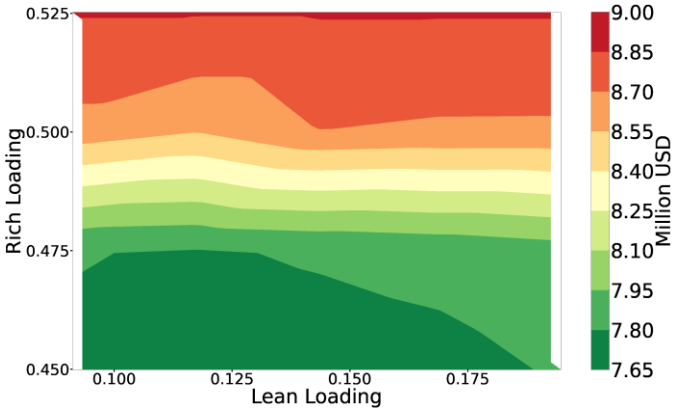

Figure 3.3.1 – CAPEX for RULCV CCS.

The contours show that the minimum CAPEX occurs at a low rich loading and a lean loading between 0.1 and 0.125. Rich loadings at the 0.525 level have unrealistic CAPEX because absorber columns larger than 100 m will not have reasonable prices. The OPEX for these columns are shown in Figure 3.3.2.

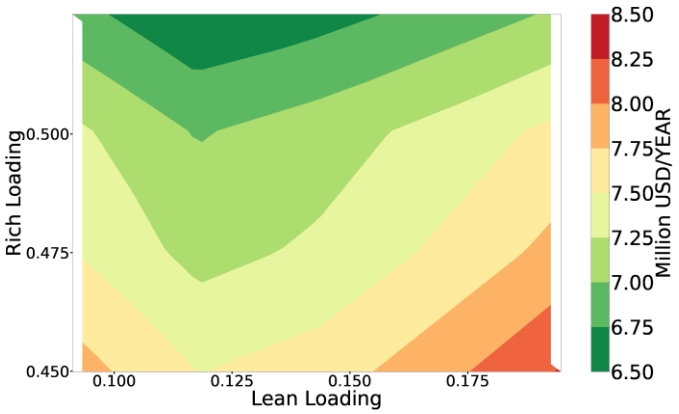

Figure 3.3.2 – OPEX for RULCV CCS.

The OPEX shows that higher rich loadings and lower lean loadings, until a critical lean loading, are favorable for minimum OPEX. Combining the annualized CAPEX with the OPEX in accordance with Equation 2.4.1 and dividing this cost by the annual CO_2 capture generates the CCC shown in Figure 3.3.3.

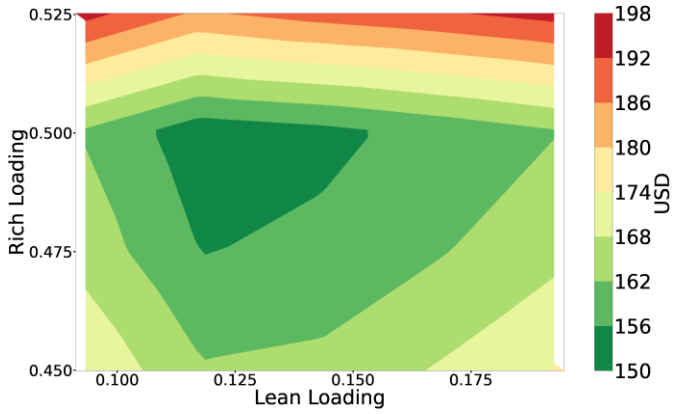

Figure 3.3.3 – CCC for RULCV CCS per ton CO_2.

There is a minimum in the CCC with lean and rich loadings of approximately 0.13 and 0.5 respectively. As lean or rich loading increase or decrease, the CCC increases. This corresponds with the steep increase in absorber height for rich loadings above 0.5, and the decreased effectiveness of reboiler duty to strip CO_2 from the amine an lean loadings below 0.13. In practice, these are the highest and lowest rich and lean loadings, respectively, that can be considered for the operation of a carbon capture system employing MEA based carbon capture at a stripper pressure of 2.5 bar and an absorber pressure of 1 bar.

3.4 Ship categories comparison

The stripper diameters for small crafts, utility vessels, cargo vessels, container ships, and the RULCV are shown in Figure 3.4.1.

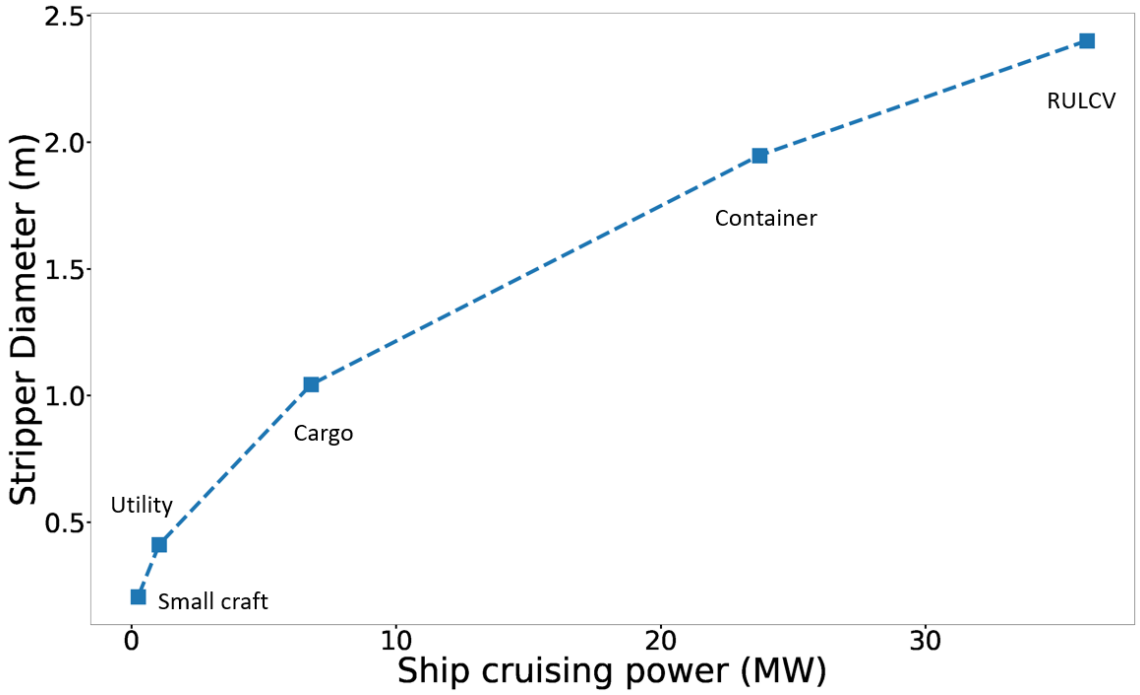

Figure 3.4.1 – Stripper diameter for ship categories.

The relationship between power and diameter is a root function. A similar behavior is observed with the absorber diameter shown in Figure 3.4.3. both of these behaviors are due to the simple fact that the flow rate of the gaseous phases in the stripper scales linearly with ships power. This is because for a constant lean-rich loading pair, amine flow rate scales directly with flue gas flow rate and reboiler duty scales directly with amine flow rate.

The linear relationship between ship power and reboiler duty is shown in Figure 3.4.2. With all flow parameters and scaling linearly with ship power, the required cross-sectional area scales directly with ships power which generates a quadratic relationship between ship power and diameter.

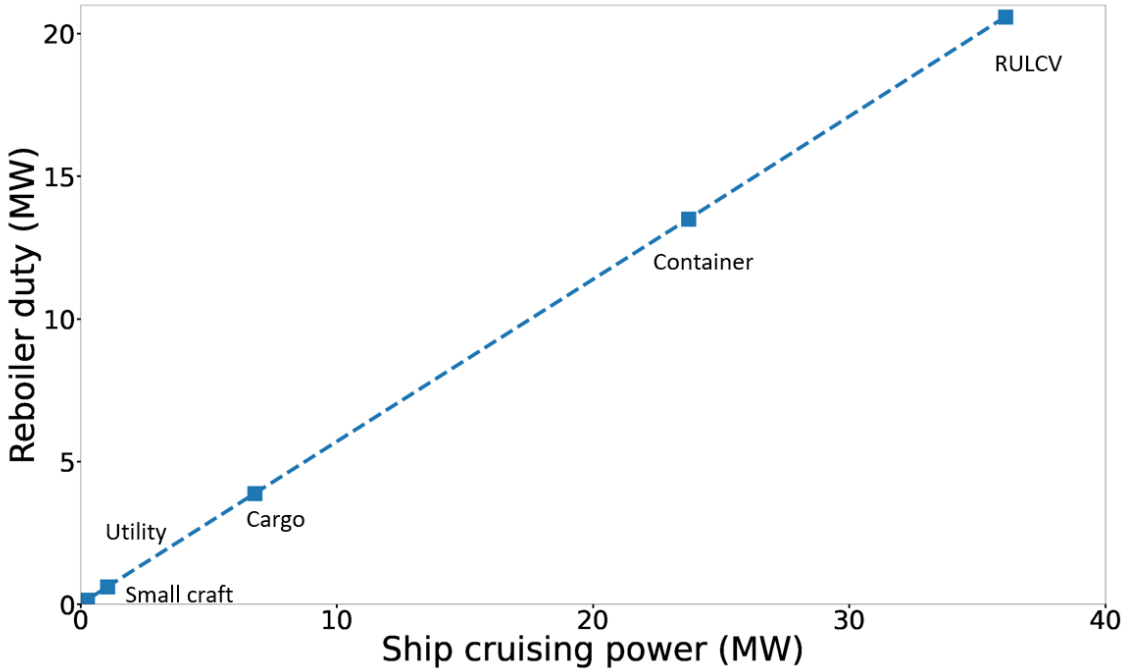

Figure 3.4.2 - Reboiler duty as a function with respect to total ships' power shows a linear relationship indicating that reboiler duty scales directly with the ship's cruising power.

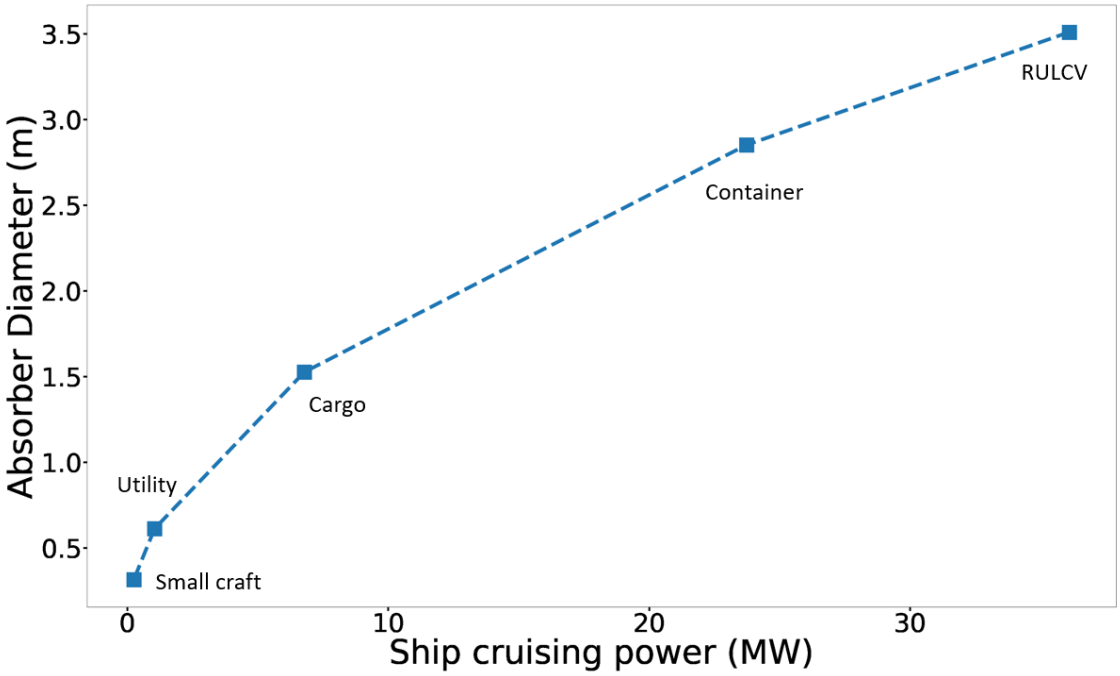

Figure 3.4.3 – Absorber diameter for ship categories.

The absorber heights are not shown because they are all the same height of 27.85 m +/- 0.1 m. In the process of sizing the absorbers, the largest absorber was sized for height and diameter to satisfy the 90% capture and 80% flooding criteria. The initial design for each subsequent smaller absorber had the same height and a diameter scaled proportionally according to the flue gas flow rate entering the column. This new diameter with the original height satisfied the 90% capture and the 80% flooding criteria exactly to within 0.1%. Since the efficiency of each stage (the determining factor in the total height needed for the absorber) is based on the percentage approach to flooding, surface effects against the packing, and the concentrations of species (rate law), the efficiencies and resulting heights for each column designed are the same. With the same structured packing, the same amine loadings, the same flue gas composition, and the 80% approach to flooding, all factors that affect stage efficiency are identical and thus return the same needed height. To explain

slight deviations yielding marginally shorter heights for the smaller diameters, the surface area of the column circumference may increase overall interfacial area per unit volume (surface area to volume ratio). Combining all sized components, the CCC for the ship categories are calculated and shown in Figure 3.4.4.

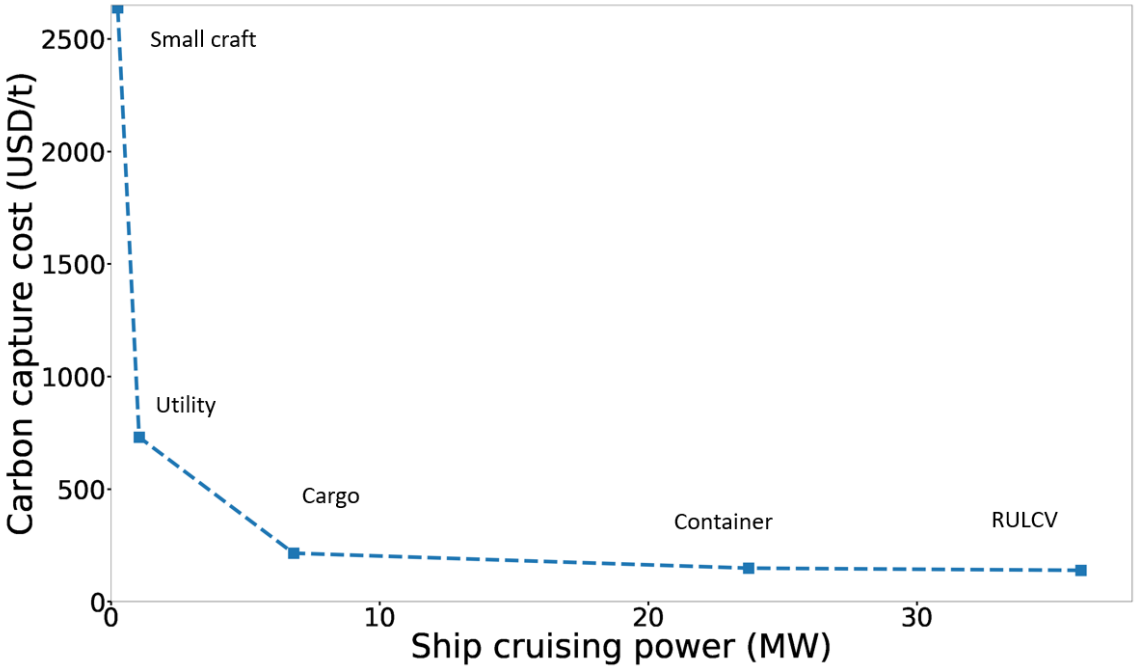

Figure 3.4.4 – CCC for ship categories.

The CCC is increases exponentially for smaller ships. This is a manifestation of economies of scale where operations become more efficient as the "overheard" costs are distributed across a larger "service". Here, the overhead costs are the upfront capital expenditures, the costs of monitoring a complex chemical plant (OPEX), and any other start-up costs considered in the installation (CAPEX) costs. The breakdown of system CAPEX, OPEX, utilities, and annualized CAPEX (ACAPEX) are shown in Figure 3.4.5.

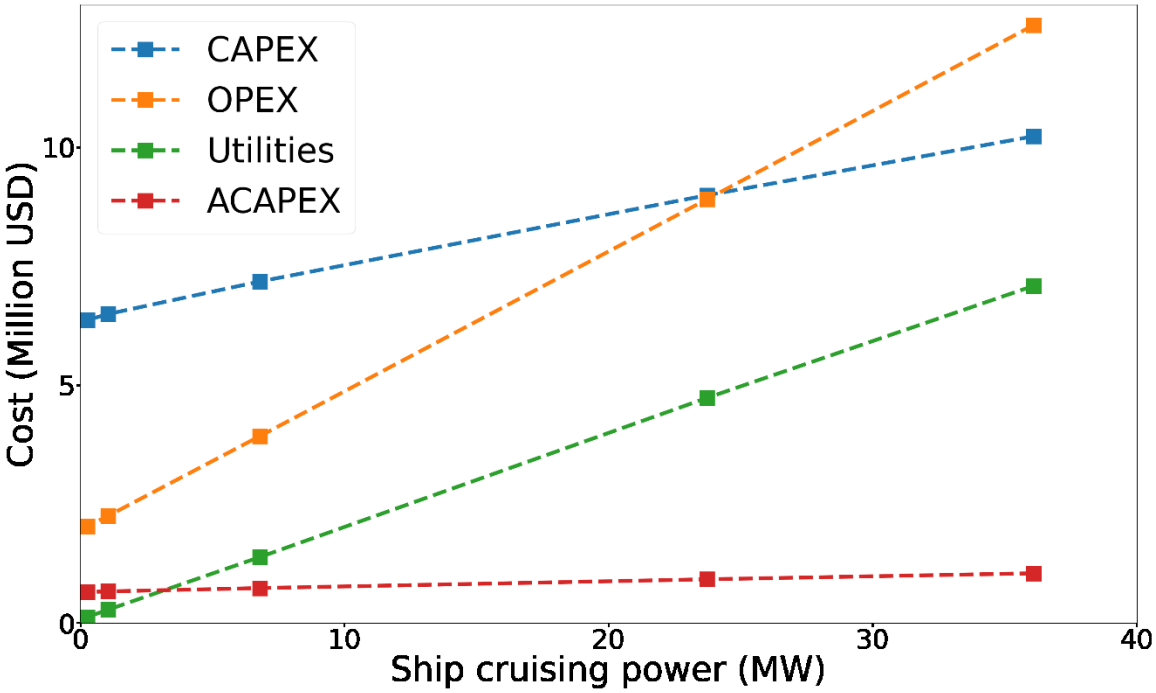

Figure 3.4.5 – Breakdown of costs associated with acquiring and operating a shipboard carbon capture system based on data from Aspen Plus Analyzer.

The minimum CAPEX, for a 256 kW ship, is still greater than six million USD. This is a massive upfront cost for the relatively small amounts of CO_2 that will be capture if such a system were installed. These CAPEX then scale linearly making larger systems more expensive but cheaper in terms of carbon capture cost.

4 Discussion

4.1 RULCV stripper

The reboiler duty on the RULCV is a strong function of amine flow rate until lean loading is below the critical loading of 0.13. At lower amine loading deltas, more amine solution must be circulated through the system. By cycling more amine solution with lower amine loading deltas, a larger proportion of the heat duty is spent reheating water as opposed to desorbing CO_2. At higher amine loading deltas, a larger fraction of reboiler heat will contribute to CO_2 desorption thus decreasing the energy required to capture CO_2 and contributing towards a reduced OPEX. Below the critical lean amine loading; however, further reductions of the lean amine loading increase reboiler duty. This minimum in reboiler duty can be attributed to CO_2 desorption below a critical value requiring more energy.

The same factors governing reboiler duty with respect to amine loading affect stripper diameter. Higher amine loading deltas require less amine solution flow which in turn requires a smaller diameter to accommodate. Below the critical lean loading, more water is heated and evaporated which increases the volume of gas flowing up the stripper column thus requiring a larger diameter to maintain an 80% approach to flooding. For both the reboiler duty and stripper diameter, the Langmuir isotherm helps explain the transition behavior in terms of occupied CO_2 binding site extinction.

4.2 RULCV absorber

The height of the absorber is almost exclusively a function of rich amine loading. This is a result of CO_2 absorption being much faster when the MEA is at a leaner loading than when it is at higher loadings. This means that changes in lean amine loading are negligible with respect to the absorber height. Conversely, changes in rich amine loading amplify changes in the absorber column height and they are a large determining factor in the total height. At a pressure of 2.5 bar, the amine loading would asymptotically approach the maximum rich amine loading in a column of infinite height. The closer to this maximum rich amine loading, the greater affect changes in the rich loading will have on the required height of the column.

The absorber diameter is governed mostly by the amine solution flow rate when evaluated at constant flue flow rates. At greater amine loading deltas, smaller diameters are needed and vice versa.

4.3 Emma Maersk economic analysis

The CAPEX is mostly determined by the size of installed components. Absorber height dominates CAPEX because beyond rich amine loadings of 0.5, the cost of such massive absorbers becomes infeasible. In addition to the shorter heights, the CAPEX shown in Figure 3.3.1 indicates a preference for lower lean loadings. The lower lean loadings provide for lower flow rates and smaller diameters.

OPEX are governed by reboiler duty. The energy required to heat and desorb CO_2 is huge compared with pump work and any other operating expenses. In Figure 3.3.2 both higher rich loadings and the critical lean loading provide a minimum operating expense.

Combining the OPEX and CAPEX in Figure 3.3.3, the OPEX contributes more towards determining the ideal lean loading while the CAPEX contributes to eliminating the feasibility of higher rich amine loadings. The two strongest governing factors in the CCC are the reboiler duty and the absorber column height. The range of the CCC per ton of CO_2 is on the same order as data in literature. CCC for amine based carbon capture have been reported at 77.5-163.07 and 100-140 €/ton CO_2 [8, 9].

4.4 Ship categories

By comparing ships of smaller sizes, it is evident that capital and operating expense decrease more slowly than CO_2 emissions decrease. This leads to an estimated CCC per ton of CO_2 in excess of $2,600/ton CO_2 for the smallest ship category considered. The utility ships category has a similarly prohibitive CO_2 capture cost of over $700/ton CO_2. The cargo and container ship categories are more feasible at CCC of $148 and $138 per ton of CO_2.

4.5 Limitations

With a parameter space this large, the limitations of any parametric study on column design will be numerous. Many of the design variable that are set can be optimized. The stripper height, the stripper pressure, and condenser temperature were not varied and those

variables all play a role in determining the operating costs. Further, a constant temperature was set for the stripper inlet temperature (95 °C) and this estimate is conservative. Here it is assumed that the reboiler duty is a direct utility cost paid for in kWh; however, much of this heat can be extracted from the flue gas on larger vessels.

It should also be noted that the OPEX and CAPEX have been calculated assuming promising conditions. Estimations for column installations do not account for the increased costs of installing onboards ships in a shipyard. While column dimensions are sized and discussed, the effects of these installations on ships are not evaluated. Furthermore, costs of lost revenue for retrofit, installation, and space onboard the ship are not considered.

4.6 Future work

Future work should explore the chemical parameter space and also consider other popular CO_2 adsorption chemicals such as piperazine and diethanolamine (DEA). In addition to various chemicals and their optimal loadings (determined by chemical equilibrium reactions), this lean / rich amine loading study for MEA can be further refined. More lean-rich loading pairs, a wider parameter sweep, and flue gas compositions from various fuels (heavy fuel oil (HFO) and liquified natural gas (LNG) instead of only diesel) should also be tested. With methane reducing best practices, LNG has the potential to reduce green-house gas emissions by 10 to 27% when compared with conventional fuels [38]. These reductions would be compounded in tandem with shipboard carbon capture [38].

In terms of physical components and parameters, many improvements can be made to this study. The heat exchanger feeding the stripper pre-heated the rich amine to 95 °C which is an overly conservative estimate leading to excessively high reboiler duties. Connecting the heat exchanger to the stripper directly should be done to more accurately predict the reboiler duty. Reboiler duty is also increased by reduced absorber temperatures. A value from literature of 40 °C was selected for the absorber temperature; however, this assumption may not be optimal and should be compared with higher and lower absorber temperature. The compressor, a critical component, should be simulated more thoroughly. The shortcut methods used simulate CO_2 compression that generates 100 bar CO_2 gas at over 400 °C; however, the temperatures would not be as high in a multistage compressor that more realistically compresses the gas. In addition to the CO_2 compression, storage must also be considered for size and weight considerations onboard a ship. Aspen Plus is not optimized for sizing of storage tanks, so these calculations should be conducted separately to be combined with data from Aspen Plus to get a more wholistic view of the carbon capture system.

With respect to shipboard installation, future extensions include optimization of layout onboard container vessels, ship stability considerations, and overall effect on the ship. The installation costs in this study are exactly what Aspen plus predicts for a land-based installation and no considerations are made to account for this increased cost of installing these large complex systems on a floating platform. The downtime required to install extra systems, and the reduced capacity also need to be accounted for in the cost of shipboard carbon capture.

To analyze the overall total effect of these systems if installed on all ships in the ULCV, a thorough list of ships and their power outputs can be acquired from databases such as Marinetraffic.com. Using this information and general data from these case studies or more detailed ones, the total percent reduction in maritime shipping emissions can be estimated.

5 Conclusions

The potential for shipboard carbon capture is significant. Every day, thousands of ULCVs, tankers, and other large ships emit hundreds of tons of CO_2 into the atmosphere. Aspen Plus offers a robust way to design and size carbon capture systems for these shipboard applications. Key design parameters for these systems include choice of amine, design lean and rich amine loadings, operating pressures, and component temperatures. Using the Aspen Plus Economic Analyzer, the cost of such installations is estimated to be on the order of $100 to $200 per ton of CO_2 captured for larger vessels (Figure 3.3.3, Figure 3.4.4).

Future studies are needed to refine these predictions, but overall they are in within the range of values estimated in literature [8, 9]. In addition to economic considerations, actual installation layouts and designs must be developed to further evaluate feasibility of such systems. The small proof of concept carbon capture system being installed onboard a Japanese coal carrier should offer insight into overall feasibility and it will likely spur larger projects if it is deemed successful [10]. The future for this mature technology is promising, though full implementation will be determined by the overall cost of carbon capture, the lower the better.

6 Acknowledgements

I thank my family for supporting me through the challenges of conducting remote research and my advisor, Betar Gallant for excellent mentorship and support.

7 Appendices

Table 4.6.1 – Mole fraction inputs for stripper rich loadings

	0.45	0.475	0.5	0.525	0.55
MEA	0.011022	0.005456	0.0011	0.0011	0.0011
H2O	0.89	0.89	0.8888	0.8834	0.878
CO2	0	0	0	0	0
H2S	0	0	0	0	0
H3O+	0	0	0.0006	0.0033	0.006
OH-	0	0	0	0	0
HCO3-	0	0	0.0006	0.0033	0.006
CO3-2	0	0	0	0	0
HS-	0	0	0	0	0
S-2	0	0	0	0	0
MEAH+	0.053988	0.057024	0.0594	0.0594	0.0594
MEACOO-	0.04499	0.04752	0.0495	0.0495	0.0495

8 References

1. Kanellos, F.D., *Optimal GHG Emission Abatement and Aggregate Economic Damages of Global Warming.* IEEE Systems Journal, 2017. **11**(4).
2. Hofmann, D., *The exponential increase in anthropogenic atmospheric carbon dioxide and its relation to human population growth*, in *American Meteorological Society*. 2009: Phoenix.
3. *Fourth IMO greenhouse gas study 2020*, in *GHG Study*. 2020: London. p. 30.
4. The White House., *President Biden Sets 2030 Greenhouse Gas Pollution Reduction Target Aimed at Creating Good-Paying Union Jobs and Securing U.S. Leadership on Clean Energy Technologies*, in *Building on Past U.S. Leadership, including Efforts by States, Cities, Tribes, and Territories, the New Target Aims at 50-52 Percent Reduction in U.S. Greenhouse Gas Pollution from 2005 Levels in 2030*. 2021.
5. *Paris Agreement*. 2015, United Nations: Paris.
6. *Paris Agreement - Status of Ratification*. 2021 [cited 2021; Available from: https://unfccc.int/process/the-paris-agreement/status-of-ratification. .
7. Minnehan, J., *Practical Application Limits of Fuel Cells and Batteries for Zero Emission Vessels*, in *Sandia Report*. 2017, Sandia National Laboratories: Albuquerque.
8. Xiaobo Luo, M.W., *Study of solvent-based carbon capture for cargo ships through process modelling and simulation.* Applied Energy, 2017. **195**: p. 402-413.

9. Maartje Feenstraa, J.M., Joan T. van den Akkerb, Mohammad R.M. Abu-Zahrac, and E.G. Erwin Gillinga, *Ship-based carbon capture onboard of diesel or LNG-fuelled ships.* International Journal of Greenhouse Gas Control, 2019. **85**: p. 1-10.
10. *Mitsubishi Shipbuilding to Test World's First Marine-based CO_2 Capture System*, in *"CC-OCEAN" project in partnership with "k" line and classnk part of japan government initiative to support development of marine resource technologies*. 2020, Mitsubishi Heavy Industries.
11. Koperna, G.J., *Project Assessment and Evaluation of the Area of Review (AoR) at the Citronelle SECARB Phase III Site, Alabama USA.* Energy Procedia, 2014. **63**: p. 5971-5985.
12. *EMMA MAERSK Container Ship, IMO: 9321483, MMSI: 220417000*. 2012 [cited 2021; Available from: https://www.vesselfinder.com/ship-photos/2889.
13. Turbo, D., *Basic principles of ship propulsion*. 2011: Man.
14. Gendre, L., *Strategies for emissions reductions in shipping: Assessing CO_2 mitigation technologies*, I.M.O. Technology, Editor. 2020.
15. Reif, K., *Diesel Engine Management Systems and Components*. 2014, Springer Vieweg: Wiesbaden. p. 329.
16. Zhang, Y., *Modeling CO2 absorption and desorption by aqueous monoethanolamine solution with Aspen rate-based model.* Energy Procedia, 2013. **37**: p. 1584-1596.
17. Vega, F., *Solvents for Carbon Dioxide Capture, Carbon Dioxide Chemistry, Capture and Oil Recovery*. 2018: IntechOpen.

18. Lv, B., *Mechanisms of CO_2 capture into monoethanolamine solution with different CO_2 loading during the absorption/desorption process.* Environmental Science and Technology, 2015. **49**: p. 10728-10735.

19. Towler, G., *Chemical Engineering Design: Principles, Practice and Economics of Plant and Process Design*. 2013, Butterworth-Heinemann: New York.

20. *Structured Packings for Distillation, Absorption and Reactive Distillation*. Sulzer.

21. Koch-Glitsch. *Model TP905, TS905 Weir Riser Pan Distributor*. 2021; Available from: https://koch-glitsch.com/Products/Packing-and-Internals/tower-internals/plastic-packed/liquid-distributors/Model-TP905,-TS905-Weir-Riser-Pan-Distributor?productcategory=Packing-and-Internals&categoryname=p-Liquid-Distributors&product=true&level=5.

22. AspenTech, *Rate-Based Model of the CO_2 Capture Process by MEA using Aspen Plus.* Aspen Plus, 2014.

23. Alger, J., *Corporate governance and the environmental politics of shipping.* Global Governance, 2021. **27**: p. 144-166.

24. Boyang Xue, Y.Y., Jian Chen, Xiaobo Luo, Meihong Wang, *A comparative study of MEA and DEA for post-combustion CO2 capture with different process configurations.* Int J Coal Sci Technol, 2016. **4**(1): p. 15-24.

25. Ajibola, B.K., *Optimization of Flooding in an Absorption-Desorption Unit*, in *Technology and Business, Kokkola*. 2010, Central Ostrobothnia University of Applied Sciences. p. 66.

26. Richardson, J.F., *Chemical Engineering: Particle technology and separation processes*. 5 ed. Vol. 2. 2002: Butterworth-Heinemann.

27. Lowenstein, J.G., *Sizing distillation.* Industrial and Engineering Chemistry, 1961. **53**(10): p. 44A-45A.

28. Mangalapally, H.P., *Pilot Plant Experiments for Post Combustion Carbon Dioxide Capture by Reactive Absorption with Novel Solvents.* Energy Procedia, 2011. **4**: p. 1-8.

29. Lim, Y., *Modeling and Simulation of CO2 Capture Process for Coalbased Power Plant using Amine Solvent in South Korea* Energy Procedia, 2013. **37**: p. 1855-1862.

30. Li, B.-H., *Simulation and analysis of CO2 capture process with aqueous monoethanolamine solution.* Applied Energy, 2016. **161**: p. 707-717.

31. Harbou, I.v., *Modeling and simulation of reactive absorption of CO2 with MEA: Results for four different packings on two different scales.* Chemical Engineering Science, 2014. **105**: p. 179-190.

32. Hüser, N., *A comparative study of different amine-based solvents for CO2-capture using the rate-based approach.* Chemical Engineering Science, 2017. **157**: p. 221-231.

33. Chia-Wen Hsieh, C.F., *Biofuels for the marine shipping sector An overview and analysis of sector infrastructure, fuel technologies and regulations*. 2017, Imternational Energy Agency Bioenergy. p. 29.

34. Neveux, T., *A Rigorous Optimization Method of Operating Parameters for Amine-Based CO2 Capture Processes.* Energy Procedia, 2013. **37**: p. 1821-1829.

35. Thibaut Neveuxa, Y.L.M., Jean-Pierre Corrioub, Eric Favre, *A Rigorous Optimization Method of Operating Parameters for Amine-Based CO$_2$ Capture Processes.* Energy Procedia, 2013. **37**: p. 1821-1829.

36. *Carbon dioxide capture handbook*, ed. N.E.T. Laboratory. 2015: U.S. Department of Energy.

37. Zumdahl, S., *Chemical Principles*. 7 ed. 2013, Belmont, CA: Brooks/Cole Cengage Learning.

38. Baroudi, H.A., *A review of large-scale CO_2 shipping and marine emissions management for carbon capture, utilization, and storage.* Applied Energy, 2021. **287**.